# Creation of Quantum Error Correcting Codes in the Ultrastrong Coupling Regime

T. H. Kyaw,[1] D. A. Herrera-Martí,[1,2] E. Solano,[3,4] G. Romero,[3] and L. C. Kwek[1,5,6]

[1]*Centre for Quantum Technologies, National University of Singapore, 3 Science Drive 2, Singapore 117543*
[2]*Racah Institute of Physics, The Hebrew University of Jerusalem, Jerusalem 91904, Israel*
[3]*Department of Physical Chemistry, University of the Basque Country UPV/EHU, Apartado 644, E-48080 Bilbao, Spain*
[4]*IKERBASQUE, Basque Foundation for Science, Maria Diaz de Haro 3, 48013 Bilbao, Spain*
[5]*Institute of Advanced Studies, Nanyang Technological University, 60 Nanyang View, Singapore 639673*
[6]*National Institute of Education, Nanyang Technological University, 1 Nanyang Walk, Singapore 637616*

(Dated: September 26, 2014)

We propose to construct large quantum graph codes by means of superconducting circuits working at the ultrastrong coupling regime. In this physical scenario, we are able to create a cluster state between any pair of qubits within a fraction of a nanosecond. To exemplify our proposal, creation of the five-qubit and Steane codes are demonstrated. We also provide optimal operating conditions with which the graph codes can be realized with state-of-the-art superconducting technologies.



*Introduction*.—Quantum computers promise speedup and robust computational power over their classical counterparts [1, 2]. However, their practical realization is still challenging due to errors susceptibility. Thanks to quantum error correcting codes (QECCs) [3, 4] and the theory of fault-tolerant quantum computation [5], these errors can, in principle, be suppressed and corrected in efficient manners. At present, the simplest quantum error correcting code that has been experimentally demonstrated [6, 7], is the three-qubit code. However, this code is not a fully quantum code because it cannot simultaneously correct both phase-flip and bit-flip errors, while the smallest QECC is the five-qubit code, that has not been experimentally demonstrated so far.

On the road towards realizing the five-qubit code and other complex codes, circuit quantum electrodynamics (cQED) architectures [8] present themselves as a prime candidate for implementing QECCs due to their high level of controllability [9, 10] and scalability [11, 12]. For instance, a recent theoretical work exploits advantages of cQED to propose autonomous quantum error correction [13], which is an important task for real-time syndrome detection and correction [14, 15]. Furthermore, it has been shown both theoretically [16] and experimentally [17, 18] that a flux qubit galvanically coupled to a coplanar waveguide resonator reaches the ultrastrong coupling (USC) regime of light-matter interaction, where the qubit-resonator coupling strength $g$ is comparable to the resonator frequency $\omega$ i.e., $0.1 \lesssim g/\omega \lesssim 1$, enabling direct application of ultrafast two-qubit gates [19] between any pair of qubits, aiming to realize complex quantum codes for quantum error correction schemes in a scalable manner.

Here, we show how to construct two QECCs, the five-qubit code [2] and the Steane code [4], in a superconducting circuit architecture operating at the USC regime. We construct them by sequentially performing ultrafast controlled phase gates ($U_{\mathcal{CZ}} = \mathrm{diag}(1, 1, 1, -1)$) between any two physical qubits to encode one logical qubit. Ultrafast gate time and high fidelity response of the superconducting circuit might ensure very low errors incurred at the logical qubit level (see *"Errors and decoherence model"* section). We believe this scheme could be used to mediate interactions between logical qubits and perform protected quantum computations in a measurement-based manner [20]. In addition, our proposal may pave a way to construct various types of QECC applications [21, 22].

*Superconducting circuit design*.—In order to achive ultrafast quantum gate operations in between any two physical qubits, we design our superconducting qubit as shown in Fig. 1(a). It consists of six Josephson junctions (JJs) each denoted with a cross. Each flux qubit is galvanically coupled [17, 18] to a coplanar waveguide resonator by means of a coupling junction, $\mathrm{JJ}_6$. This qubit configuration provides a tunable qubit-resonator coupling strength [19, 23] with the flux qubit [24] potential energy composed of JJ's 1, 2 and 3. Each JJ contributes an energy $\mathcal{E}(\varphi_i) = -E_{J_i}\cos(\varphi_i)$, where $E_{J_i}$ and $\varphi_i$ are the Josephson energy and the gauge-invariant superconducting phase difference across the $i$th junction. We assume $E_{J_1} = E_{J_2} = E_J$, $E_{J_3} = \alpha E_J$, $E_{J_4} = E_{J_5} = \beta E_J$, and the quantization rule for each closed loop, i.e., $\sum_j \varphi_j = 2\pi f_i + 2\pi n$ where $f_i = \phi_i/\Phi_0$ is a frustration parameter ($i = 1, \ldots, 5$), $\Phi_0 = h/2e$ is the flux quantum, and $n$ is an integer multiple. Near its symmetry point, i.e., $\phi_1 \approx \Phi_0/2$, the flux qubit behaves effectively as a two-level system with frequency $\omega_q = \sqrt{\Delta^2 + \varepsilon^2}/\hbar$. Here, $\Delta$ is the qubit energy gap and $\varepsilon = 2I_p(\phi_1 - \Phi_0/2)$ with $I_p$ being the persistent current.

We consider the setup in Fig. 1(c) to construct the simplest QECC, the five-qubit code, as depicted in Fig. 1(b). Since the five flux qubits are equally spaced and placed in a single-mode resonator, we find that the coupling junctions, $\mathrm{JJ}_6$'s, introduce extra boundary conditions to the resonator. Under the assumption that each $\mathrm{JJ}_6$ operates in a linear response regime, where the Josephson energy $E_J$ is much larger than the capacitive energy $E_C$, this leads to a non-linear resonator spectrum where each harmonic presents a manifold $\mathcal{M}$ whose number of frequencies corresponds to the number of qubits embedded across the resonator [25]. In this sense, the Hamiltonian of the

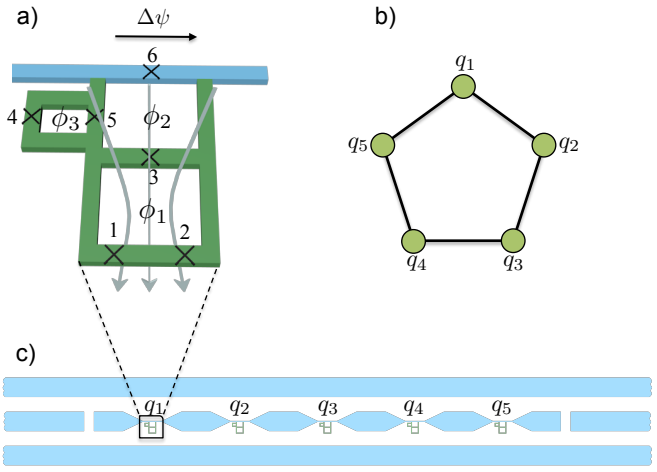


FIG. 1. (color online). a) Schematic of a flux qubit, denoted by the Josephson junctions 1, 2 and 3. By varying the frustration parameter $f_3$, attained by an applied magnetic flux passing through the loop compsed of the JJ's 4 and 5, the coupling between the qubit and the resonator can be tuned at will. This is a crucial aspect of our superconducting qubits design in order to realize cluster states in ultrafast timescale. b) A five-qubit cluster state. Each black bond represents the pair-wise cluster state generation mechanism $U_{CZ}^{ij}$ between $i$th and $j$th physical qubits (green circles) that are initially prepared in the $|+\rangle = (|0\rangle + |1\rangle)/\sqrt{2}$ state. c) An array of five USC qubits embedded in a resonator to obtain the five-qubit quantum error correcting code.

total system can be written as

$$H = \frac{\hbar}{2}\sum_{j=1}^{N}\omega_q^j\sigma_z^j + \hbar\sum_{\ell\in\mathcal{M}}\omega_\ell a_\ell^\dagger a_\ell + \hbar\sum_{j=1}^{N}\sum_{\ell\in\mathcal{M}} g_j(c_x^j\sigma_x^j + c_z^j\sigma_z^j)(a_\ell + a_\ell^\dagger), \quad (1)$$

where $\omega_q^j$ is the $j$th qubit frequency, $\sigma_{z,x}^j$ are Pauli matrices, $\omega_l$ is frequency of the $\ell$th resonator mode pertaining to the manimold $\mathcal{M}$, $a_\ell^\dagger(a_\ell)$ is the creation (annihilation) operator of the $\ell$th resonator mode, $c_x^j$ and $c_z^j$ are functions of the system parameters $\alpha, \beta, f_1$, and $f_2$ [19], satisfying the condition $|c_x|^2 + |c_z|^2 = 1$ for $\forall j$, the coupling strength $g_j \propto 2E_J\beta\cos(\pi f_3)/\hbar$, depends on the external magnetic flux $\phi_3$, and $N$ is the total number of qubits present in the resonator. We note that different coupling strengths appear due to a spatial dependence of the flux distribution along the resonator. Moreover, different frequencies belonging to a specific manifold $\mathcal{M}$ become degenerate ($\omega_\ell = \omega$) [25] for a specific value of the plasma frequency $\omega_p = 1/\sqrt{C_J L_J}$ associated with the coupling junctions, where $C_J$ is the Josephson capacitance and $L_J = \varphi_0^2/E_J$ is the Josephson inductance, where $\varphi_0 = \Phi_0/2\pi$ is the reduced flux quantum.

It is noteworthy that coefficients $c_x$ and $c_z$ can be manipulated by means of the external flux $\phi_1$ as shown in Fig. 2(a,b). Here, it might be possible to tune the transversal coupling where $c_x \to 1$ and $c_z \to 0$ or the longitudinal coupling where $c_x \to 0$ and $c_z \to 1$. The latter becomes an essential tool for the generation of pairwise cluster state generation.

*Pairwise cluster state generation.*—A cluster state between the $i$th and $j$th qubits can be generated in four steps. Firstly, the system is cooled down to reach its ground state in the USC regime. Secondly, both qubits are adiabatically addressed with external fluxes that vary linearly in time $\phi_3^k = \bar{\phi}_0 + \Delta\phi t/T$ where $k \in \{i, j\}$, with $\bar{\phi}_0$ an offset flux, $\Delta\phi$ a small flux amplitude, and $T$ total evolution time. In this case, each individual qubit reaches the strong coupling regime described by the Jaynes-Cummings model [26] such that the system is prepared in the state $|\psi_G\rangle = |g\rangle^{\otimes N}\otimes|0\rangle^{\otimes M}$, where $|g\rangle$ and $|0\rangle$ stand for the ground state of the qubit and the vacuum state for each mode in $\mathcal{M}$, respectively. Thirdly, each qubit is then addressed with a classical microwave signal, sent through the cavity, to be prepared in the state $|+\rangle = (|g\rangle + |e\rangle)/\sqrt{2}$ which is an eigenstate of $\sigma_x$, while all the remaining $N-2$ qubits are far off-resonant with respect to the driving frequency. At this stage all qubits should dispersively interact with the modes within the manifold $\mathcal{M}$ such that there is no exchange of excitations. This task might be achieved by working at the degenerate regime of the bosonic manifold, $\omega_\ell = \omega$ [25]. At last, the external magnetic fluxes $\phi_3^k$ are swiftly tuned to reach the USC coupling strength $g/\omega = 0.25$ within a subnanosecond timescale. During these four steps, the magnetic fluxes $\phi_1^k$ should be tuned to reach the longitudinal qubit-resonator coupling. After interacting with the collective resonator modes, the system evolution operator takes the form [27, 28]

$$U(t) = U_0(t)e^{i\xi^2 M(\omega t - \sin(\omega t))}\prod_l e^{-i\omega t a_\ell^\dagger a_\ell}\mathcal{D}_\ell[\kappa(t)], \quad (2)$$

where $D_\ell[\kappa(t)] = \exp[\kappa(t)a_\ell^\dagger - \kappa^*(t)a_\ell]$ is a displacement operator associated with the $\ell$th bosonic mode within the manifold $\mathcal{M}$. In addition, $\xi = \sum_{j=1}^N \kappa_j\sigma_z^j$ with $\kappa_j = g_j/\omega$, $M$ stands for the number of degenerate bosonic modes $b_\ell$, and the unitary $U_0(t) = \exp(-it\sum_{j=1}^N \frac{\omega_q^j}{2}\sigma_z^j)$. At time $T = 2\pi n/\omega$, we have performed the controlled phase gate between the two qubits

$$U_{CZ} = \mathcal{U}\times\exp\left[-\frac{i\pi}{4}(\sigma_z^i + \sigma_z^j)\right] \times\exp\left[4\pi i M\left((\kappa_i^2 + \kappa_j^2)\frac{\mathbb{I}}{2} + \kappa_i\kappa_j\sigma_z^i\sigma_z^j\right)\right], \quad (3)$$

where $\mathcal{U} = \exp\left[\frac{-i\pi}{4}\left[\left(\frac{4\omega_q^i-\omega}{\omega}\right)\sigma_z^i + \left(\frac{4\omega_q^j-\omega}{\omega}\right)\sigma_z^j\right]\right]$. Thus, we incur an extra global phase due to the presence of $\mathcal{U}$, which is unavoidable since it is formidable by construction to tune a desired qubit frequency without affecting the longitudinal and transversal coupling strengths (see Fig. 2(a) and (b)). To achive maximum fidelity for a controlled phase gate, we require both $\kappa_i^2 + \kappa_j^2 = \frac{1}{8nM}$ and $\kappa_i\kappa_j = \frac{1}{16nM}$. That means the two coupling strengths need to satisfy $\kappa_i + \kappa_j = \frac{1}{2\sqrt{nM}}$. The estimated gate time is calculated to be $T = 2\pi/\omega \sim 0.2$ns if the collective mode frequency is $\omega = 2\pi\times 5$ GHz. As soon

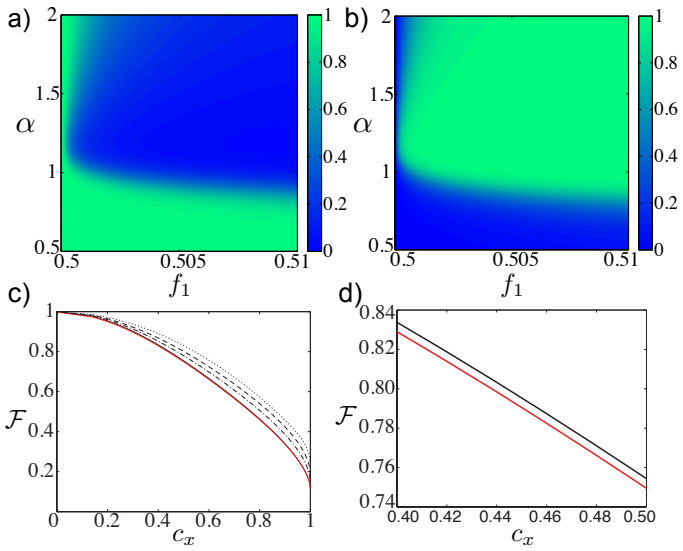


FIG. 2. (color online). Coupling coefficients a) $c_x$ and b) $c_z$ in Eq. (6) as a function $\alpha$, that is the size of junction $JJ_3$, and the frustration parameter $f_1 = \phi_1/\Phi_0$. c) Fidelity of achieving the desired controlled-phase gate $U_{\mathcal{CZ}}$, in the presence of non-zero transversal coupling strength $c_x$ while the red solid line, the black solid line, the dot-dashed line, the dashed line and the dotted line represent the case when the resonator field is a thermal state at 15mK, a vacuum state, a coherent state with amplitude $\gamma = 0.25$, a coherent state with $\gamma = 0.5$ and a coherent state with $\gamma = 1$ respectively. d) The inset figure shows the enlarged figure where the red and black solid lines do not overlap each other.

as the two qubits are entangled, they are immediately detuned from the resonant frequency so that we can repeat the same process for other pairs of qubits to arrive at a specific quantum correcting code; be it the five-qubit code (see Fig. 1(b)) or the Steane code (see Fig. 3).

*Five-qubit code*.—To demonstrate our ultrafast cluster state generation scheme, we create the five-qubit code which is the smallest QECC that protects against an arbitrary error on a single qubit encoded state [2]. We recall that a cluster state is a common eigenstate of stabilizer operators $K_i = X_i \bigotimes_{j\in nb(i)} Z_j$, where $X_i = \sigma_x^i$, $Z_i = \sigma_z^i$ and $nb(i)$ means neighbours of the $i$th qubit. Since the stabilizer operators form a group $|\psi\rangle = K_i|\psi\rangle = K_iK_j|\psi\rangle$, it is possible to define $S_i' = K_iK_{i+1 \bmod 5}$ and logical operators $\bar{X} = K_5$ and $\bar{Z} = Z_1Z_2Z_3Z_4Z_5$, from which it follows that the five-qubit cluster state is equivalent to the five-qubit code via local unitary transformation $U = \bigotimes_i S_iH_i$, where $S_i(H_i)$ is the phase (Hadamard) gate (see Ref. [29]). Therefore, we create the five-qubit cluster state shown in Fig. 1(b) by applying the pairwise cluster state generation mechanism $U_{\mathcal{CZ}}^{ij}$. The resultant state is

$$|\Psi_5\rangle = U_{\mathcal{CZ}}^{15}U_{\mathcal{CZ}}^{54}U_{\mathcal{CZ}}^{43}U_{\mathcal{CZ}}^{32}U_{\mathcal{CZ}}^{21}|+\rangle^{\otimes 5}, \tag{4}$$

after an evolution time $\tau_5 = 10\pi/\omega$. After local operations acting on individual qubits we achieve the five-qubit code.

*Steane Code*.—The Steane code [4] can also be constructed in the similar manner as the five-qubit code, but from a cluster state of ten qubits as shown in Fig. 3. We require seven stabilizer operators, among ten possible operators, in the combination of operators that commute with $X_8$, $X_9$ and $X_{10}$. It can easily be checked that measuring the orange colored qubits in the $X$ basis leaves the remaining seven qubits in the desired code state [2]. With twelve $U_{\mathcal{CZ}}^{ij}$ gates followed by three parallel measurements within an evolution time of $\tau_7 = 24\pi/\omega$, we achieve the Steane code

$$|\Psi_7\rangle = \langle+|_{10}\langle+|_9\langle+|_8 \prod_{k\in E} U_{\mathcal{CZ}}^{k}|+\rangle^{\otimes 10}, \tag{5}$$

where $E$ represents a set of all the black colored bonds in Fig. 3.

*Errors and decoherence model*.—The pairwise cluster state generation mechanism assumes that coupling coefficients $c_x^j = 0$ in Eq. (6). That means we require only longitudinal couplings. However, there might be some residual non-zero transversal couplings in an implementable situation. Whenever this is the case, i.e., $c_x^j \neq 0$, the performance of the ultrafast gate $U_{\mathcal{CZ}}$ is affected, depending on the amount of residuals. In order to see the gate performance with presence of the transversal couplings, we perform numerical calculations in Fig. 2(c,d), where we provide optimal operating conditions with which we can obtain maximum gate fidelity. Furthermore, vacuum field inside the resonator might not be truly vacuum and strayed non-vacuum field such as thermal or coherent states might be present inside the resonator, depending on how well the system can be initialized. Even though the presence of vacuum, thermal or coherent state inside the resonator at near $c_x \ll 1$ does not affect much to the gate performance, we see that coherent state field in the resonator has clear advantage over the true vacuum field (see Fig. 3(c)). Particularly, we observe improvement of the gate fidelity when the resonator field becomes closer to the classical field, i.e., for a coherent state amplitude $\gamma \to 1$.

In addition to imperfection of the resonator field and the coupling strengths, we expect that our system be exposed to

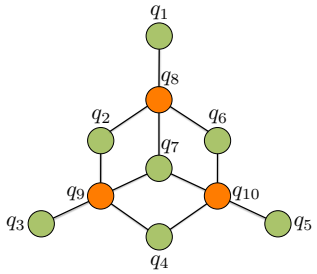


FIG. 3. (color online). A ten-qubit cluster state emerging the Steane code after appropriate projective measurements on the physical qubits $q_8$, $q_9$ and $q_{10}$ (orange circles). Each black bond represents the pair-wise cluster state generation mechanism $U_{\mathcal{CZ}}^{ij}$ between the $i$th and $j$th physical qubits (green circles) that are initially prepared in the $|+\rangle = (|0\rangle + |1\rangle)/\sqrt{2}$ state.

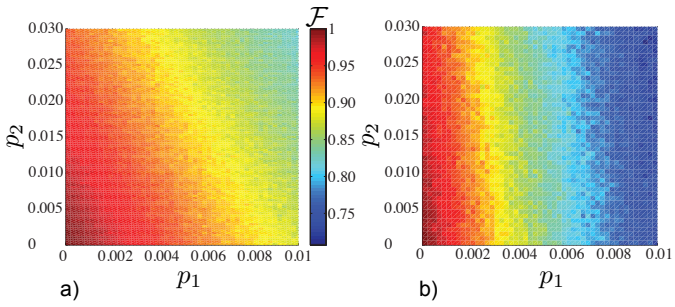


FIG. 4. (color online). Montecarlo simulation results. Fidelity of (a) the five-qubit code, where the average fidelity value is taken over 5000 runs and (b) the Steane code, where the average fidelity value is taken over 1000 runs is plotted against single-qubit gate error probability $p_1$ and two-qubit gate error probability $p_2$.

thermal noise from the control lines and crosstalks between physical qubits. We model these effects as uncorrelated depolarizing noise which follows otherwise perfect gates, and estimate fidelity of the final states by performing Montecarlo simulations for generation of the two QECCs. Also, we consider measurement error of $p_m = 0.01$ [12] for the case of the Steane code, should there be an error in the process. At the end, the collective state of the qubit can be written as $\rho = \mathcal{F}|\Psi_\nu\rangle\langle\Psi_\nu| + (1-\mathcal{F})\mathbb{I}/2^\nu$, where $\mathcal{F}$ is the fidelity of attaining the five-qubit code ($\nu = 5$ and see Fig. 4(a)) or the Steane code ($\nu = 7$ and see Fig. 4(b)).

*Discussions*.—In summary, we have proposed a possible realization of the five-qubit and the Steane codes in an array of superconducting circuits galvanically coupled to a coplanar waveguide resonator that mediates two-qubit interactions. The system operates in the USC regime, in which two-qubit gates of subnanosecond timescale are demonstrated. At this timescale, it is strenuous for the gate errors to be limited by the coherence time of the qubit and the resonator in the galvanic configuration [17, 18], whose rough estimation is $10-100$ ns and $160-500$ ns, respectively [30]. However, recent randomized benchmarking techniques in circuit QED technologies [9, 11] have shown that the error per gate can be reduced to about $0.5\%$. This precedent might encourage the realization of our approach in which case fidelities in excess of $75\%$ could be achieved. Also, imperfect measurements are significant sources of errors in the construction of cluster states. However, extremely fast measurements with $99\%$ fidelity have been demonstrated in Ref. [12]. Thus, we believe our proposal, with all the advanced technologies in the superconducting circuits, might pave a promising avenue for implementing large scale QECCs or topological codes [31] in ultrafast timescale.

This work was supported by the National Research Foundation, the Ministry of Education, Singapore; Spanish MINECO FIS2012-36673-C03-02; UPV/EHU UFI 11/55; Basque Government IT472-10; SOLID, CCQED, PROMISCE, and SCALEQIT European projects.

[1] R. P. Feynman, Int. J. Theor. Phys. **21** 467 (1982); P. W. Shor, Foundations Computer Sci. 12 (IEEE, 1994); L. K. Grover, Phys. Rev. Lett. **79** 325 (1997).
[2] M. A. Nielsen and I. L. Chuang, *Quantum Computation and Quantum Information* (Cambridge University Press, Cambridge, 2000).
[3] P. W. Shor, Phys. Rev. A. **52**, R2493 (1995).
[4] A. M. Steane, Phys. Rev. Lett. **77**, 793 (1996).
[5] D. Gottesman, Phys. Rev. A. **57**, 127 (1998).
[6] J. Chiaverini, D. Leibfried, T. Schaetz, M. D. Barrett, R. B. Blakestad, J. Britton, W. M. Itano, J. D. Jost, E. Knill, C. Langer, R. Ozeri, and D. J. Wineland, Nature **432** 602 (2004).
[7] M. D. Reed, L. DiCarlo, S. E. Nigg, L. Sun, L. Frunzio, S. M. Girvin, and R. J. Schoelkopf, Nature **482** 382 (2012).
[8] A. Blais, R.-S. Huang, A. Wallraff, S. M. Girvin, and R. J. Schoelkopf, Phys. Rev. A. **69** 062320 (2004); A. Wallraff, D. I. Schuster, A. Blais, L. Frunzio, R.- S. Huang, J. Majer, S. Kumar, S. M. Girvin, and R. J. Schoelkopf, Nature **431**, 162 (2004); I. Chiorescu, P. Bertet, K. Semba, Y. Nakamura, C. J. P. M. Harmans, and J. E. Mooij, Nature **431**, 159 (2004).
[9] R. Barends et al., Nature **508**, 500 (2014).
[10] Y. Chen et al., arXiv:1402.7367.
[11] J. M. Chow, J. M. Gambetta, E. Magesan, S. J. Srinivasan, A. W. Cross, D. W. Abraham, N. A. Masluk, B. R. Johnson, C. A. Ryan, and M. Steffen, Nature Comm. **5**, 4015 (2014).
[12] E. Jeffrey et al., Phys. Rev. Lett. **112**, 190504 (2014).
[13] J. Cohen and M. Mirrahimi, arXiv:1409.6759.
[14] J. Kerckhoff, H. I. Nurdin, D. S. Pavlichin, and H. Mabuchi, Phys. Rev. Lett. **105**, 040502 (2010).
[15] J. Kerckhoff, D. S. Pavlichin, H. Chalabi, and H. Mabuchi, New J. Phys. **13**, 055022 (2011).
[16] J. Bourassa, J. M. Gambetta, A. A. Abdumalikov, Jr., O. Astafiev, Y. Nakamura, and A. Blais, Phys. Rev. A **80**, 032109 (2009).
[17] T. Niemczyk, F. Deppe, H. Huebl, E. P. Menzel, F. Hocke, M. J. Schwarz, J. J. Garcia-Ripoll, D. Zueco, T. Hümmer, E. Solano, A. Marx, and R. Gross, Nature Phys. **6**, 772-776 (2010).
[18] P. Forn-Díaz, J. Lisenfeld, D. Marcos, J. J. García-Ripoll, E. Solano, C. J. P. M. Harmans, and J. E. Mooij, Phys. Rev. Lett. **105**, 237001 (2010).
[19] G. Romero, D. Ballester, Y. M. Wang, V. Scarani, and E. Solano, Phys. Rev. Lett. **108**, 120501 (2012).
[20] H. J. Briegel and R. Raussendorf, Phys. Rev. Lett. **86**, 5188 (2003).
[21] R. Ozeri, arXiv:1310.3432.
[22] G. Arrad, Y. Vinkler, D. Aharonov, and A. Retzker, Phys. Rev. Lett. **112** 150801 (2014).
[23] B. Peropadre, P. Forn-Díaz, E. Solano, and J. J. García-Ripoll, Phys. Rev. Lett. **105**, 023601 (2010).
[24] T. P. Orlando, J. E. Mooij, L. Tian, Caspar H. van der Wal, L. S. Levitov, S. Lloyd, and J. J. Mazo, Phys. Rev. B. **60** 15398 (1999).
[25] M. Leib and M. J. Hartmann, arxiv:1402.1325.
[26] E. T. Jaynes and F. W. Cummings, Proc. IEEE **51**, 89 (1963).
[27] See supplemental material, which presents the full derivation of the evolution operator $U(t)$, and includes Refs. [13,16,20,22].
[28] Y. D. Wang, S. Chesi, D. Loss, and C. Bruder, Phys. Rev. B **81**, 104524 (2010).
[29] D. A. Herrera-Martí and T. Rudolph, Quant. Inf. Comp. **13**, 0995 (2013).
[30] Private communications.
[31] E. Dennis, A. Landahl, A. Kitaev, and J. Preskill, J. Math.

Phys. **43** 4452 (2002); R. Raussendorf, J. Harrington, and K. Goyal, Ann. Phys. **321** 2242 (2006); D. S. Wang, A. G. Austin, and L. C. L. Hollenberg, Phys. Rev. A. **83** 020302(R) (2011); R. Raussendorf and J. Harrington, Phys. Rev. Lett. **98** 190504 (2007); S. D. Barrett and T. M. Stace, Phys. Rev. Lett. **105** 200502 (2010).

## SUPPLEMENTARY INFORMATION

### DERIVATION OF THE EVOLUTION OPERATOR

For the system shown in Fig. 1(c) of the main text, and a system-alike with $N$ flux qubits equally spaced and galvanically coupled [1] with a resonator line, we have shown in the main manuscript that these systems can be modeled as

$$H = \frac{\hbar}{2}\sum_{j=1}^{N}\omega_q^j\sigma_z^j + \hbar\sum_{\ell\in\mathcal{M}}\omega_\ell a_\ell^\dagger a_\ell + \hbar\sum_{j=1}^{N}\sum_{\ell\in\mathcal{M}} g_j(c_x^j\sigma_x^j + c_z^j\sigma_z^j)(a_\ell + a_\ell^\dagger). \quad (6)$$

It has been shown that magnetic fluxes $\phi_1$'s can tune the coefficients $c_x$ and $c_z$ (see Fig. 2(a,b) of the main text) to arrive at the longitudinal coupling with $c_x \approx 0$ and $c_z \approx 1$ [2, 3], which is an ideal condition for the pairwise cluster state generation in an ultrafast timescale. For each mode $\ell$, we define a displacement operator

$$\mathcal{D}_\ell(\sum_j \kappa_j\sigma_z^j) = \exp[(\sum_j \kappa_j\sigma_z^j)a_\ell^\dagger - (\sum_j \kappa_j\sigma_z^j)a_\ell], \quad (7)$$

with $\kappa_j = g_j/\omega$ and $\omega_\ell = \omega$ since we consider a collective resonator mode at a degeneracy point [4]. In addition, for all the modes within the manifold $\mathcal{M}$, we define a collective displacement operator

$$\mathcal{D}(\xi) = \prod_{\ell\in M} e^{\xi a_\ell^\dagger - \xi^* a_\ell}, \quad (8)$$

where $\xi = \left(\sum_j \kappa_j\sigma_z^j\right)$. By transforming the original Hamiltonian, Eq. (6), with the above operator, we obtain

$$\begin{aligned} H &= \mathcal{D}^\dagger(\xi)\mathcal{D}(\xi)H\mathcal{D}^\dagger(\xi)\mathcal{D}(\xi) \\ &= \mathcal{D}^\dagger(\xi)[\omega\sum_\ell a_\ell^\dagger a_\ell - \omega M\xi^2]\mathcal{D}(\xi), \end{aligned} \quad (9)$$

where $M$ is the dimension of $\mathcal{M}$. The associated evolution operator is given by

$$\begin{aligned} U(t) &= U_0(t)e^{i\omega tM\xi^2}e^{-i\omega t\mathcal{D}^\dagger(\xi)(\sum_\ell a_\ell^\dagger a_\ell)\mathcal{D}(\xi)} \\ &= U_0(t)e^{i\xi^2M(\omega t - \sin(\omega t))}\prod_l e^{-i\omega t a_\ell^\dagger a_\ell}\mathcal{D}_\ell\big[\xi(t)\big], \end{aligned} \quad (10)$$

with $U_0(t) = \exp[-it\sum_j \frac{\omega_q^j}{2}\sigma_z^j]$ and $\mathcal{D}_\ell\big[\xi(t)\big] = \mathcal{D}_\ell((1 - e^{i\omega t})\xi)$. After an evolution time $t = 2\pi n/\omega$,

$$U(2\pi n/\omega) = U_0(2\pi n/\omega)e^{i\xi^2M(2\pi n)}\prod_\ell e^{-2\pi n i a_\ell^\dagger a_\ell}, \quad (11)$$

where $n$ is an integer multiple. Since our protocol constitutes pairwise qubits,

$$\begin{aligned} U(2\pi/\omega) \approx \exp[\frac{-i\pi}{\omega}(\omega_q^i\sigma_z^i + \omega_q^j\sigma_z^j)] \\ \exp[i4\pi nM((\kappa_i^2 + \kappa_j^2)\frac{\mathbb{I}}{2} + \kappa_i\kappa_j\sigma_z^i\sigma_z^j)]. \end{aligned} \quad (12)$$

Thus, we have

$$\begin{aligned} U_{\mathcal{CZ}} &= \mathcal{U}\times\exp\left[\frac{-i\pi}{4}(\sigma_z^i + \sigma_z^j)\right] \\ &\times\exp\left[4\pi iM\left((\kappa_i^2 + \kappa_j^2)\frac{\mathbb{I}}{2} + \kappa_i\kappa_j\sigma_z^i\sigma_z^j\right)\right], \end{aligned} \quad (13)$$

where $\mathcal{U} = \exp\left[\frac{-i\pi}{4}\left[\left(\frac{4\omega_q^i-\omega}{\omega}\right)\sigma_z^i + \left(\frac{4\omega_q^j-\omega}{\omega}\right)\sigma_z^j\right]\right]$ and $n = 1$. To perform the controlled phase gate with a maximum fidelity, we require that both $\kappa_i^2 + \kappa_j^2 = \frac{1}{8nM}$ and $\kappa_i\kappa_j = \frac{1}{16nM}$ are satisfed. In other words, we need $\kappa_i + \kappa_j = \frac{1}{2\sqrt{nM}}$.

[1] J. Bourassa, J. M. Gambetta, A. A. Abdumalikov, Jr., O. Astafiev, Y. Nakamura, and A. Blais, Phys. Rev. A **80**, 032109 (2009).
[2] G. Romero, D. Ballester, Y. M. Wang, V. Scarani, and E. Solano, Phys. Rev. Lett. **108**, 120501 (2012).
[3] B. Peropadre, P. Forn-Díaz, E. Solano, and J. J. García-Ripoll, Phys. Rev. Lett. **105**, 023601 (2010).
[4] M. Leib and M. J. Hartmann, arxiv:1402.1325.